

## Structural, Morphological and Electrochemical Impedance Study of CS:LiTf based Solid Polymer Electrolyte: Reformulated Arrhenius Equation for Ion Transport Study

Shujahadeen B. Aziz<sup>1,2,\*</sup>, M. F. Z. Kadir<sup>3</sup>, Z. H Z. Abidin<sup>4</sup>

<sup>1</sup> Advanced Materials Research Lab., School of Science-Department of Physics, Faculty of Science and Science Education, University of Sulaimani, Sulaimani, Kurdistan Regional Government-Iraq

<sup>2</sup> Development Center for Research and Training (DCRT), University of Human Development, Orga Street, Sulaimani, Kurdistan Regional Government-Iraq.

<sup>3</sup> Centre for Foundation Studies in Science, University of Malaya, 50603 Kuala Lumpur, Malaysia

<sup>4</sup> Department of Physics, Faculty of Science, University of Malaya, 50603 Kuala Lumpur, Malaysia

\*E-mail: [shujaadeen78@yahoo.com](mailto:shujaadeen78@yahoo.com)

Received: 31 July 2016 / Accepted: 3 September 2016 / Published: 10 October 2016

This paper discusses ion conduction mechanism in terms of reformulated Arrhenius equation. Understanding the fundamental concepts of Li ion transport is crucial for Li battery technology. Structural and morphological investigations are significant to understand the structure-properties relationships. The broadening of X-ray peaks of chitosan upon the addition of LiTf salt reveals that the crystalline domains are reduced. The SEM micrographs reveal that the samples have a smooth surface. Electrochemical impedance spectroscopy (EIS) was used to obtain the electrical and dielectric parameters. The dielectric constant and DC ionic conductivity follows the same trend with salt concentration. The behavior of Arrhenius and modified Arrhenius equations versus temperature are clarified. The influence of dielectric constant on DC conductivity experimentally achieved. The

reformulated Arrhenius equation ( $\sigma_{(\epsilon',T)} = \sigma_o \exp\left(\frac{-E_a}{K_B \epsilon' T}\right)$ ) exhibited more linearity between the DC conductivity and  $1000/(\epsilon' \times T)$ . The shortcoming of Arrhenius equation can be understood from the less linear behavior of DC conductivity versus  $1000/T$ . The pre-exponential factor is almost constant at different temperature and independent on dielectric constant. The calculated activation energy from the reformulated Arrhenius equation is greater than that obtained from Arrhenius equation.

**Keywords:** Polymer electrolyte; XRD and SEM analysis; Dielectric constant and DC conductivity; reformulated Arrhenius equation.

### 1. INTRODUCTION

The progress of harmless electrolytes is one of the leading subjects in the field of secondary lithium batteries research. In particular solid polymer electrolytes (SPEs), represent one of the hottest topics, despite this class of compounds being introduced already almost forty years ago [1]. SPEs can be produced by combination polar polymers with alkali metal salts and ion transport through such membranes occurs when an external electric field is applied [2]. Polar polymer materials containing electron donating atoms with low dissociation energy alkali metal salts give electrolytes for advanced electrochemical devices, e.g. batteries/fuel cells, electrochemical display devices/smart windows and photoelectrochemical cells [3]. These polymer electrolytes offer many important properties such as fast cation transport combined with plasticity [4], satisfactory mechanical properties, ease of fabrication as thin films, high electrochemical stability and ability to form good electrode/electrolyte contact [3]. The cations are weakly coordinated to sites along the polymer chain and they can transfer from one coordinated site to another. A lot research effort has since then been directed toward understanding the complex chemistry and ionic transport properties of these technologically important materials [5, 6]. Ionic conduction in SPEs is known to take place in the amorphous fraction of the polymer matrix, but the polymers used as hosts in polymer electrolytes are often semi-crystalline [7, 8]. Recently Malathi et al., [9], and Prajapati et al., [10], have considered complex permittivity parameters in explaining ionic conductivity of PVA based solid polymer electrolytes. Pradhan et al., [11, 12], and Sengwa et al., [13], have also used dielectric analysis to understand the conductivity behavior in nano-composite solid polymer electrolytes. On the other hand, Kadir et. al., [14], used the scanning electron microscope (SEM) to detect the leakage of un dissolved salts in Chitosan:PVA: $x\text{NH}_4\text{NO}_3$  system. They achieved the fact that the smooth and homogeneous surface can be ascribed to a good miscibility of the system. In our previous works we used successfully the SEM technique to detect the leakage of silver nanoparticles in silver ion conducting polymer electrolytes and their effect on optical and electrical properties [15, 16]. The extensive and intensive survey of literature indicated that very little work has been done on dielectric properties of ion conducting solid polymer electrolytes [7]. Even the mechanism of ion conduction in SPEs is still not well understood. Hence, it becomes important to understand the ion transport behavior in solid polymer electrolytes. This work is different from previous works on polymer electrolytes in which they focused on conductivity enhancement. The goal of the current work is to interpret the ion transport mechanism from the electrical and dielectric relationships. In this study we show empirically the necessary of reformulation of Arrhenius equation. Furthermore, from the estimated activation energy the role of dielectric constant on ionic conductivity can be understood. To support the electrical results the XRD and SEM technique has been carried out to establish structure-properties relationships. In the present work low salt concentration has been used to distinguish the electrode polarization region from the bulk (high frequency semicircular) region.

## 2. EXPERIMENTAL METHOD

### 2.1 Materials and sample preparation

Chitosan (CS) from crab shells ( $\geq 75\%$  deacetylated, Sigma aldrich) and lithium triflate (LiTf) with a molecular weight 256.94 (supplied by Fluka,  $\geq 98$  purity) have been used as the raw materials in

this study. The solid polymer electrolyte (SPE) films were prepared by the solution cast technique with acetic acid (1%) as a solvent. In the present work 1 gm of chitosan was fixed and dissolved in acetic acid solution. The mixture was stirred at room temperature for 24 hours until a homogeneous solution were obtained. To the prepared chitosan solution, lithium triflate (LiCF<sub>3</sub>SO<sub>3</sub>) was incorporated and varied from 2 wt. % to 10 wt. % in steps of 2wt. % to prepare various composition of CS:LiTF electrolyte in weight percent ratios; 100:0 for pure chitosan acetate (CSC1), 98:2 (CSC2), 96:4(CSC3), 94:6(CSC4), 92:8(CSC5) and 90:10 (CSC6) for CS:LiTF. This procedure produces a homogeneous electrolyte solution. After casting in different plastic Petri dish, the solutions were left to dry at room temperature for films to form. The films were transferred into a desiccator for continuous drying.

2.2 X-Ray Diffraction analysis

In this paper, XRD was performed to show the occurrence of complex formation between LiCF<sub>3</sub>SO<sub>3</sub> and chitosan. The XRD pattern of pure chitosan and doped chitosan films were recorded using X-ray (1.5406 Å) diffractometer (Bruker AXS) with operating voltage and current of 40 kV and 40 mA, respectively. The glancing angles were in the range of 5° ≤ 2θ ≤ 80° with a step size of 0.1°.

2.3 Morphological analysis

The scanning electron micrograph (SEM) is an important technique to understand the morphological changes especially surface morphology. A scanning electron micrograph was taken using Leica 440 scanning electron microscope to study morphological appearance [7]. Before observation, the CS:LiTf solid polymer electrolyte films were attached to aluminum holder using a conductive tape, and then coated with a thin layer of gold.

2.4 Impedance measurement

The electrical behavior of pure CS and CS:LiTf solid films were measured using the HIOKI 3531 Z Hi-tester which is interfaced to a computer in the frequency range from 50 Hz to 1000 kHz. For this purpose the pure CS and CS:LiTf solid films were cut into small discs of 2 cm diameter and sandwiched between two stainless steel electrodes under spring pressure. The intersection of Z' on the real part of complex impedance was used to calculate the DC ionic conductivity as follows [17],

$$\sigma_{DC} = \left[ \left( \frac{1}{Z'} \right) \times \left( \frac{l}{A} \right) \right] \dots\dots\dots (1)$$

Whrer *l*, is the sample thickness, *Z'* is the resistance and *A* is the electrode area (cm<sup>2</sup>). The real (*Z'*) and imaginary (*Z''*) part of complex impedance (*Z\**) were used for calculate the real part of complex permittivity (*ε\**) using the following relations [7],

$$Z^* = Z' - jZ'' \tag{2}$$

$$\varepsilon^* = \varepsilon' - j\varepsilon'' = \frac{1}{j\omega\varepsilon_0 Z^*} \quad (3)$$

From equation (1) and equation (2) one can get the following relation,

$$\varepsilon' = \frac{Z''}{\omega C_0 (Z'^2 + Z''^2)} \quad (4)$$

where  $C_0$  is the vacuum capacitance, given by  $\varepsilon_0 A/l$ , where  $\varepsilon_0$  is the permittivity of free space. The angular frequency  $\omega$ , is equal to  $\omega = 2\pi f$ , where  $f$  is the frequency of applied field.

### 3. RESULTS AND DISCUSSION

#### 3.1 X-ray diffraction analysis

In this system, XRD was performed to show the complex formation occurrence between  $\text{LiCF}_3\text{SO}_3$  and chitosan. The crystalline peaks of pure  $\text{LiCF}_3\text{SO}_3$  can be detected at  $2\theta = 16.5^\circ$ ,  $19.75^\circ$ ,  $20.4^\circ$ ,  $22.55^\circ$ ,  $25.3^\circ$ , and  $33.15^\circ$ . The X-ray diffraction pattern and crystalline peaks of the  $\text{LiCF}_3\text{SO}_3$  salt (Fig.1) is in good agreement with literature [18]

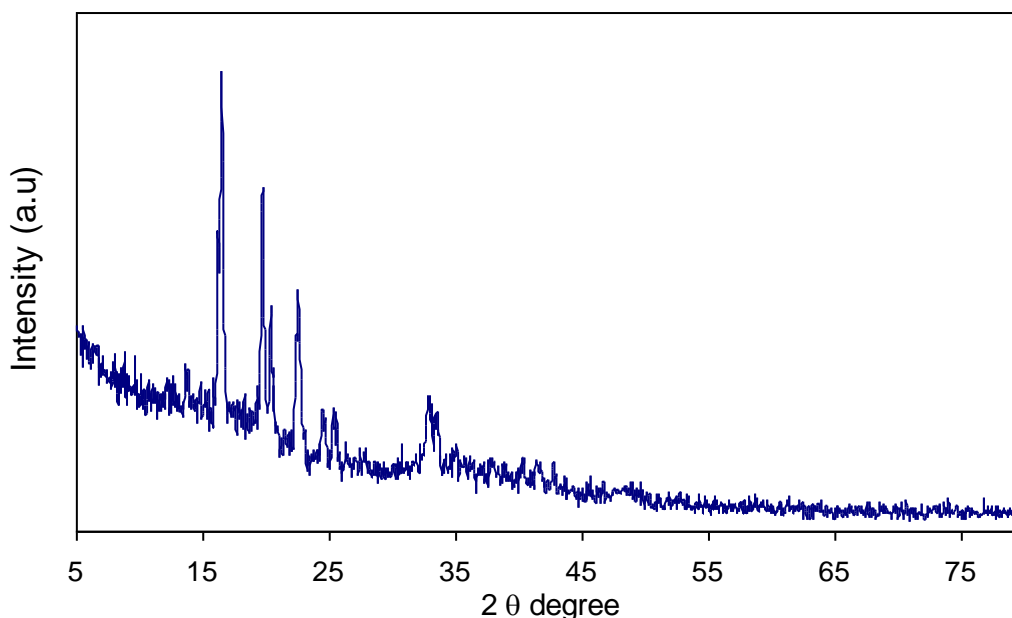


**Figure 1.** X-ray diffraction pattern of pure  $\text{LiCF}_3\text{SO}_3$  salt.

The diffractograms of the pure chitosan acetate film (CSC1) and chitosan: $\text{LiCF}_3\text{SO}_3$  complexes, are illustrated in Figure 2. It is obvious that, with addition of lithium triflate (LiTf) into chitosan matrix, intensity of the crystalline peaks of pure chitosan decreased drastically (see Fig. 2). This indicates the reduction in crystalline region of chitosan matrix [19]. The dominance of amorphous region can be expected directly from the widening of diffraction peaks and decreasing the peak

intensities of the pure polymer upon the addition of inorganic salt [7]. The reduction in crystallinity results from the complex formation between the polar groups of the polymer and the cations of the salt as a result of electrostatic interaction and thus retards the ordering of the crystalline regions in polymer electrolyte [7, 19]. The higher the amorphous nature of the electrolyte results in higher conductivity of the sample [7]. It can be seen that the peak of pure chitosan at  $15.5^\circ$  shifted to  $12.6^\circ$  in CS:LiTf systems.

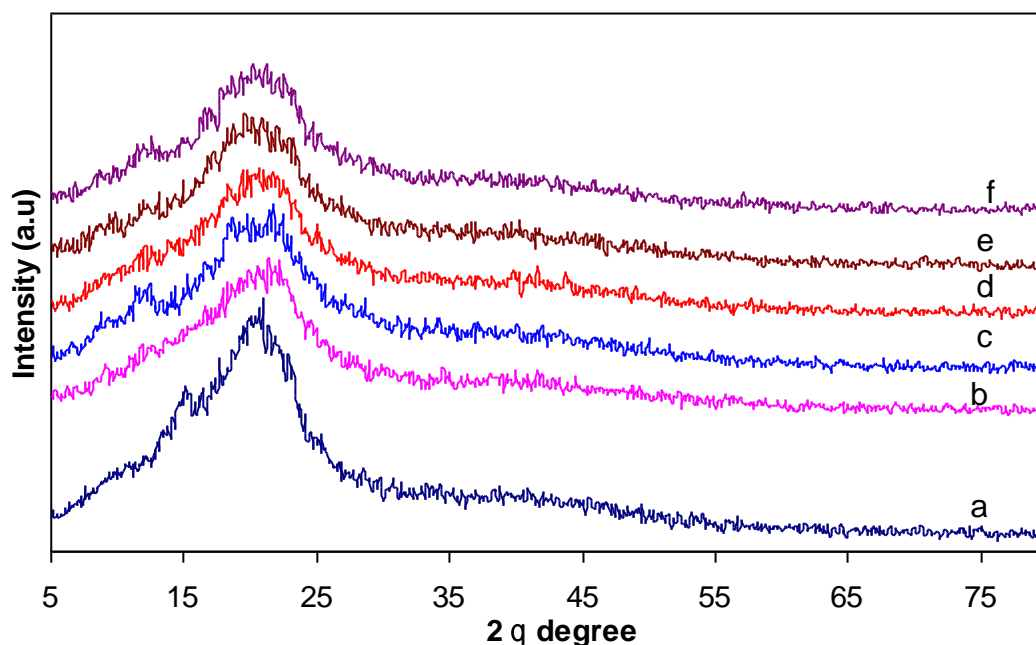


**Figure 2.** X-ray diffractogram of (a) CSC1 (pure chitosan), (b) CSC2, (c) CSC3, (d) CSC4, (e) CSC5 and (f) CSC6.

The crystalline structure of CS:LiTf solid electrolyte samples were further analyzed by using Origin 8 software. By introducing the XRD raw data to Origin 8 software the full width at half maximum (FWHM) can be achieved. From the FWHM the crystallite size was calculated using the Debye–Scherrer [18, 19]. To examine the role of LiTf salt on the crystalline structure of chitosan solid electrolyte the crystallite size of CS:LiTf electrolytes was calculated using the Debye–Scherrer formula [15]. The gaussian fitting on CSC2 (2 wt.% LiTf), CSC5 (8 wt.% LiTf) and CSC6 (10 wt.% LiTf) SPE samples were shown in Figure3. The obtained FWHM for these samples were presented in Table I. The CSC6 sample exhibits a largest FWHM value. The calculated crystallite sizes in Table 1 reveal that the CSC6 sample is more amorphous. It was well reported that it is possible to study the crystalline structure of solid and nanocomposite polymer electrolytes from the achieved crystallite sizes [15, 20-22]. The large crystallite size of CSC6 sample indicates its amorphousness.

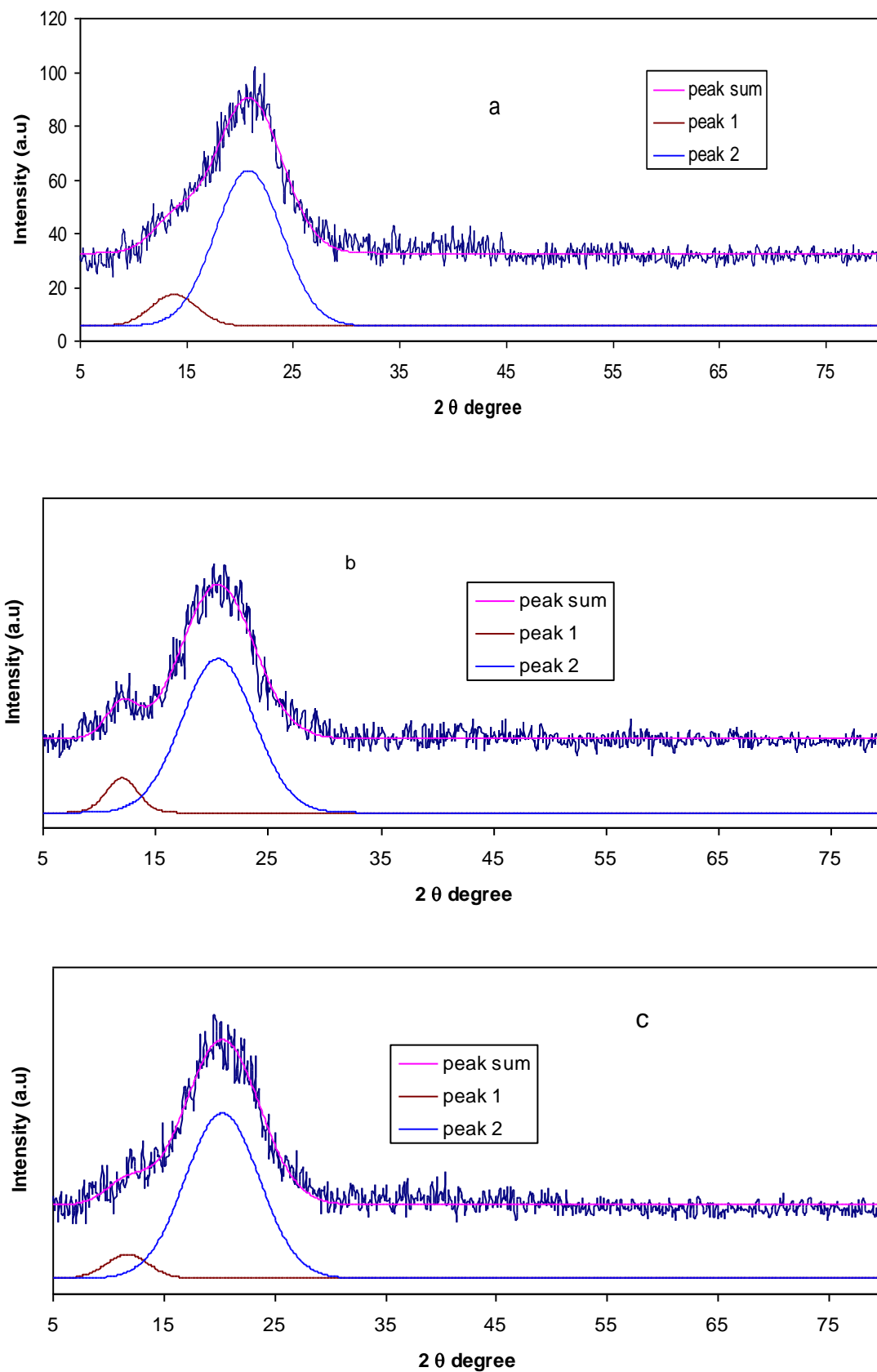
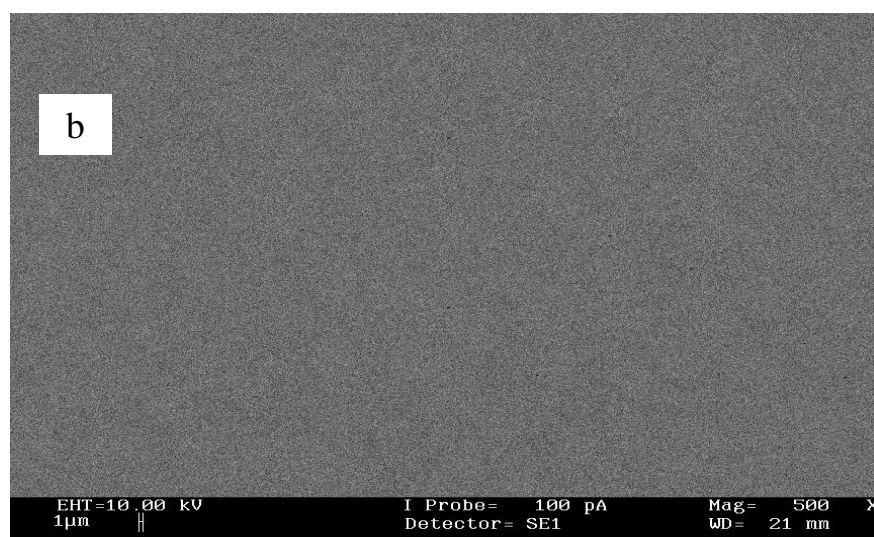
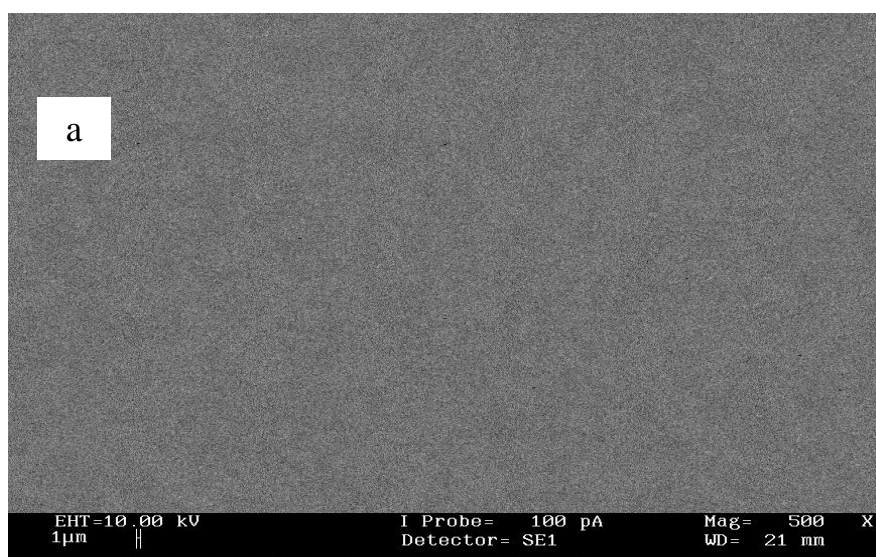


**Figure 3.** Gaussian fitting of XRD for (a) CSC2, (b) CSC5 and (c) CSC6 samples.

**Table 1.**  $2\theta^\circ$ , FWHM, and crystallite size (L) for CSC2, CSC5 and CSC6 SPEs.

Sample Designation	$2\theta$ degree	FWHM (rad)	L ( $\text{\AA}$ )
CSC2	20.8	0.108679	13
CSC5	20.5	0.111993	12.5
CSC6	20.3	0.116878	12.1

### 3.2 SEM analysis of SPEs



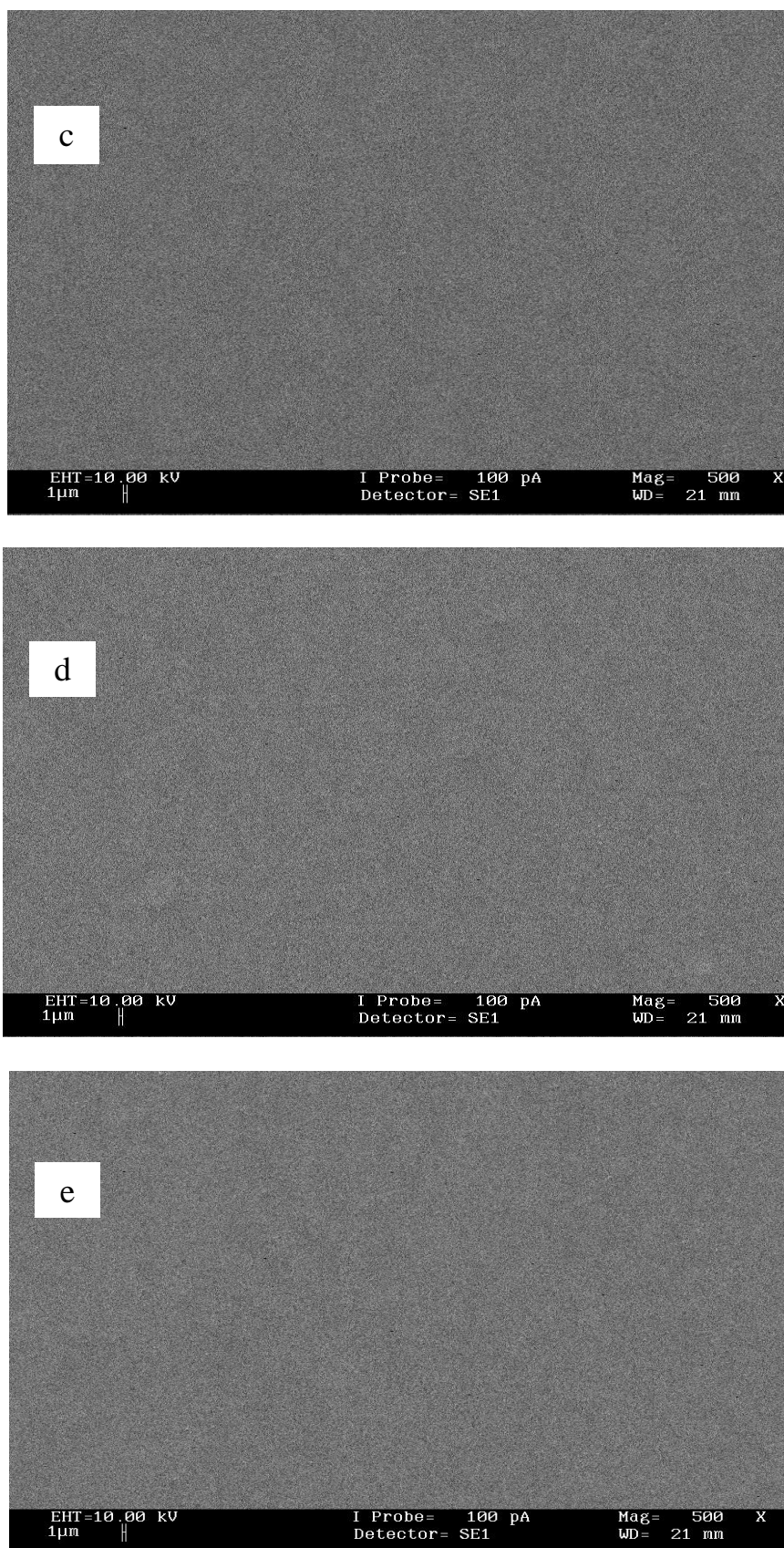


**Figure 4.** Scanning electron microscopy (SEM) image for (a) CSC2, (b) CSC3, (c) CSC4, (d) CSC5 and (e) CSC6.

SEM micrograph for the surface of the solid polymer electrolyte samples are shown in Figure 4(a-e). A uniform surface morphology can be observed for pure and CS:LiTf solid samples. The SEM characterizations were carried out in order to understand the morphological changes during LiTf addition to chitosan. The smooth surface of all the samples and the non existence of phase separation reveal a good miscibility or complex formation between CS and LiTf salt [14]. In our previous work on CS:AgTf system a lot of clusters and white chains of silver nanoparticles are appeared on the surface of the of the samples [16].

### 3.3 DC conductivity and Dielectric analysis

The main idea of this research work is to explore the correlation between DC conductivity and dielectric constant and this may opens another way to study the DC conductivity ion conducting polymer electrolytes.

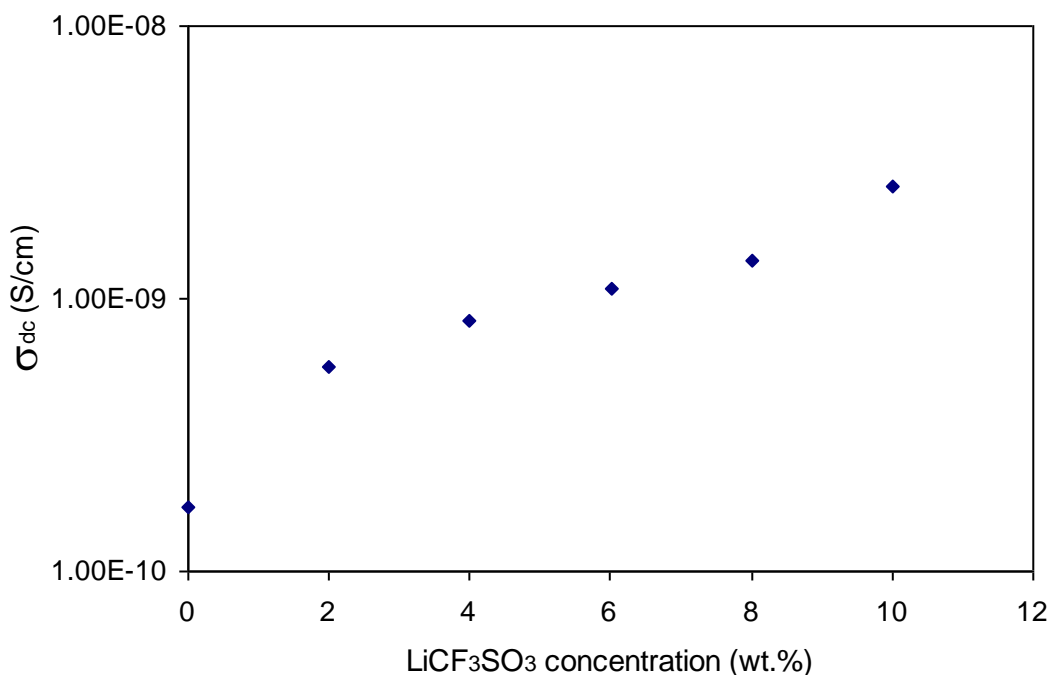


**Figure 5.** DC conductivity as a function of LiCF<sub>3</sub>SO<sub>3</sub> concentration.

The bulk DC conductivity and bulk dielectric constant are calculated from the high frequency semicircle. The reformulated Arrhenius equation and the constant behavior of pre-exponential factor ( $\sigma_0$ ) at various temperatures are checked from the existence relationships between DC conductivity and dielectric constant. Previously, Petrowsky and Frech [23, 24], assumed that the DC ionic conductivity is dependent on the dielectric constant in addition to temperatures at low salt concentration in organic liquid electrolytes. They have also interpreted the non-Arrhenian behavior of DC conductivity as a result of dependence of pre-exponential factor,  $\sigma_0$ , on the dielectric constant,

$\sigma_{(T,\epsilon')} = \sigma_{o(\epsilon'(T))} \exp(-\frac{E_a}{K_B T})$ . Figure 5 represents the DC ionic conductivity against LiTf salt concentration. It is obvious that the room temperature DC conductivity increases with increasing LiTf concentrations. The DC conductivity increment can be ascribed to the increase in charge carrier density.

Figure 6 illustrates the concentration dependence of dielectric permittivity ( $\epsilon'$ ) at different frequencies. The low frequency region (I) shows the dispersion while the high frequency region (II) is almost constant which represent the materials property. It can be noticed that the chitosan:LiCF<sub>3</sub>SO<sub>3</sub> (CSC6) sample i.e., the most amorphous sample exhibits higher  $\epsilon'$  compared to other samples.

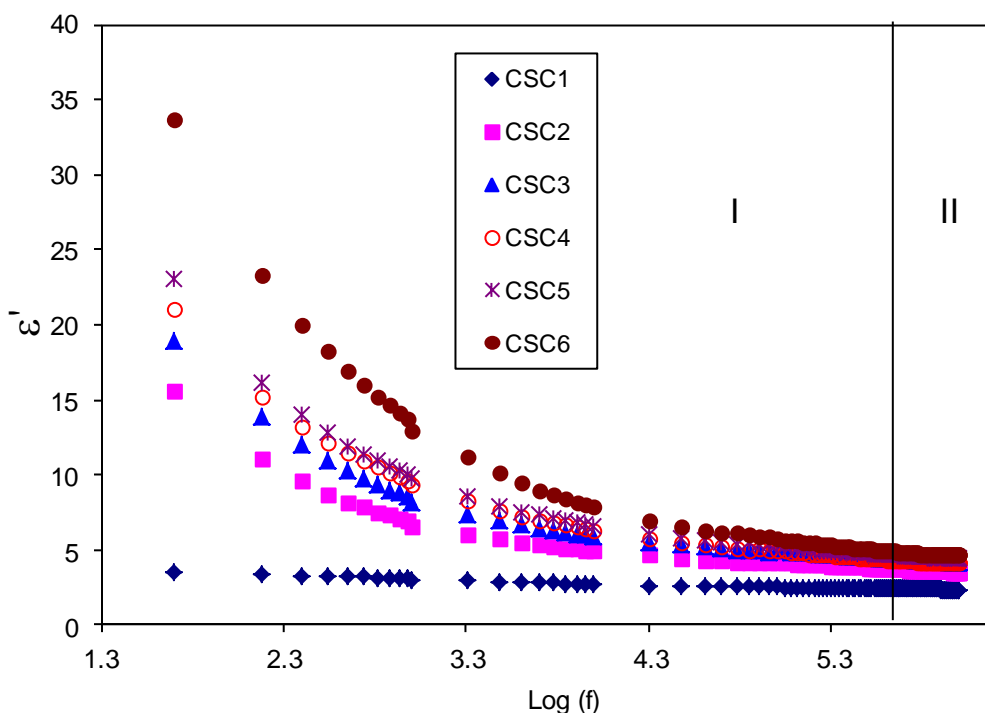


**Figure 6.** Compositional dependence of dielectric constant for CS:LiTf SPEs.

Figure 7 shows the composition dependence of bulk dielectric constant (high frequency region, II). It can be seen that the high conducting sample exhibits high dielectric constant. This can be attributed to the high cation carrier concentration. When salt dissociates into polymer matrix, it forms mobile cations and anions. Under the influence of an external electric field, ions tend to move along the the polymer chain appropriately. However, movable charge carriers are unable to cross the blocking electrode-electrolyte interface

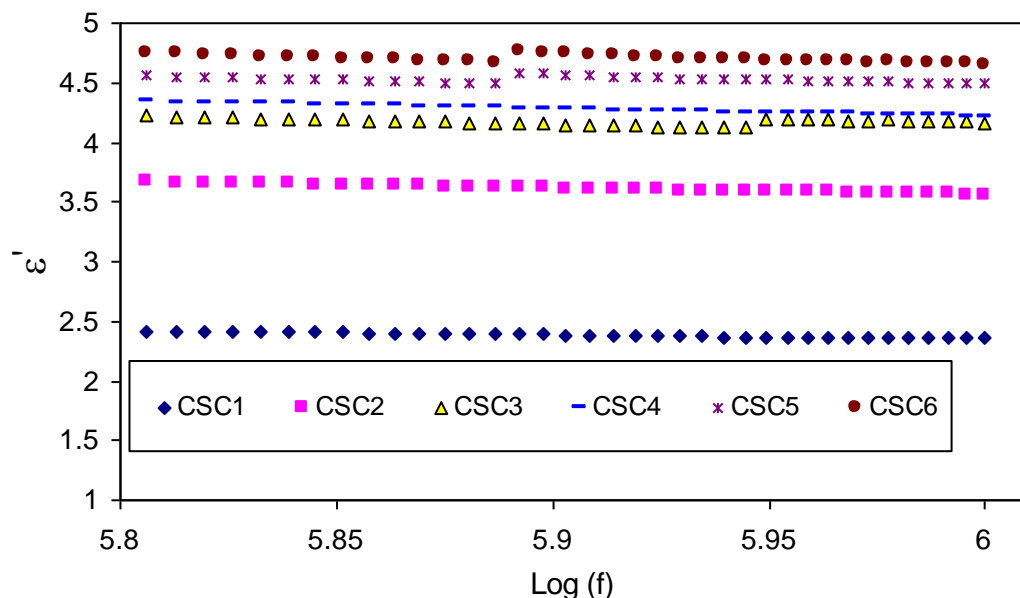


Figure 7. Compositional dependence of bulk dielectric constant for CS:LiTf SPEs.

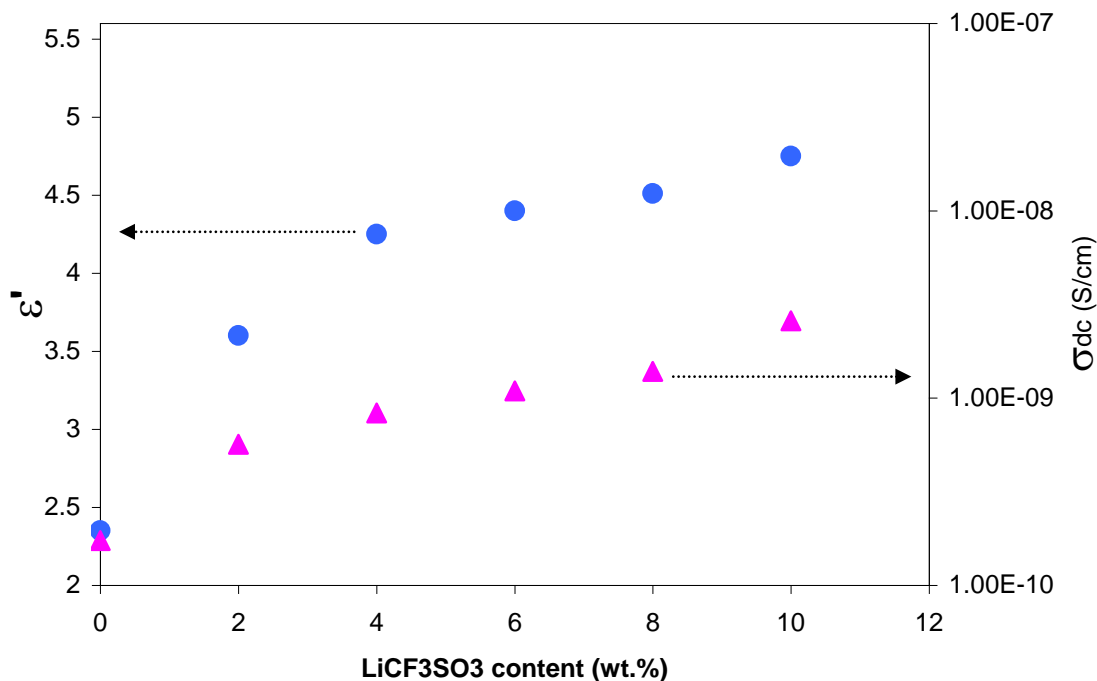


Figure 8. Variation of dielectric constant and DC conductivity with various LiTf concentrations.

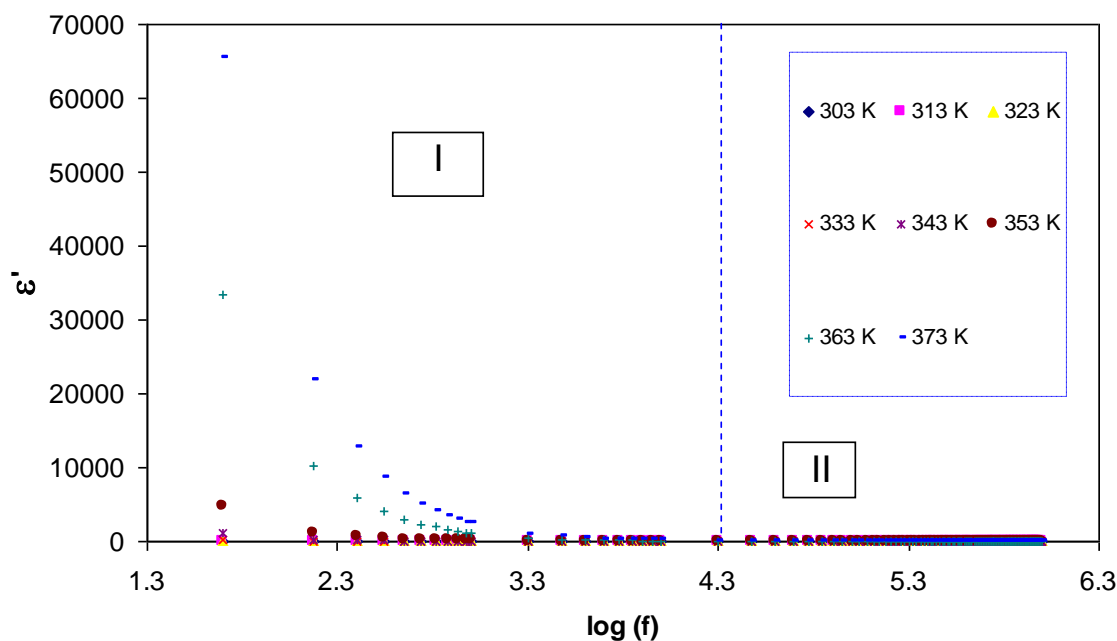
Figure 8 illustrates the bulk dielectric constant and DC conductivity as a function of salt concentration. It is clear that the behavior of  $\epsilon'$  and  $\sigma_{dc}$  with LiTf salt is the same. To date, many polymer electrolytes with wonderful conduction properties have been prepared, but the ion transport mechanism still is not well understood. The DC ionic conductivity is related to charge carriers and mobility as follows [25],

$$\sigma(T) = \sum n_i q_i \mu_i \tag{5}$$

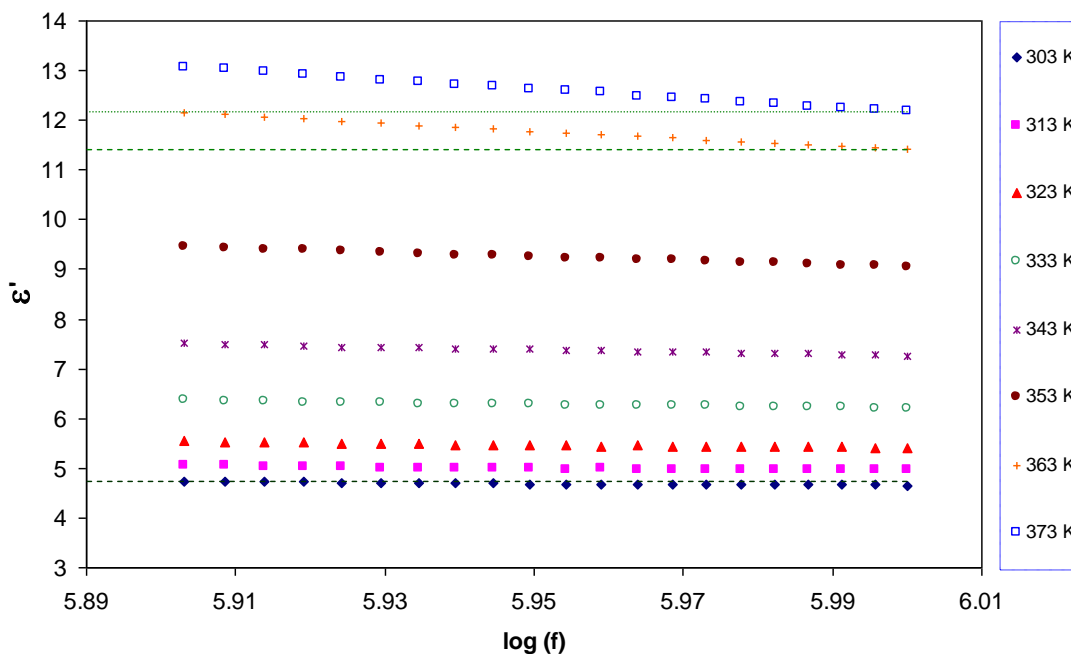
where  $n_i$  is the number density of carriers and  $q_i$  and  $\mu_i$  are the charge and mobility of the charge carriers, respectively. Both a huge amount and fast mobility of ion carriers are necessary to give good ionic conductivity. Hence, it is important to find appropriate materials that gather these necessities [25]. It is clear from the above equation that the role of dielectric constant on ion conduction mechanism is ignored.

Figure 9 exhibits the dielectric constant spectra versus frequency at different temperatures for CS:LiTf (CSC6) sample. The high value of dielectric constant at low frequency (region I) can be attributed to phenomenon of electrode polarization (EP). The high frequency region (region II) which appeared as a plateau is related to the bulk property of the sample is also temperature dependent as depicted in Figure 10. The enhancement in  $\epsilon'$  value at high temperatures indicates the increase in charge carrier concentration because dielectric constant represents the storage of charge carriers. In polar polymers, temperature can facilitates the orientation of dipoles and this result in increased permittivity ( $\epsilon'$ ) [26]. The increase in permittivity leads to dissociation of more ions that are able to participate in polarization as well as in conduction. Thus the increase of bulk dielectric constant means an increase of bulk DC conductivity because both are calculated from the high frequency semicircle. To observe the role of dielectric constant on ion transport mechanism, the DC ionic conductivity should be plotted against dielectric constant at different temperatures.

Figure 11 illustrates the DC conductivity against dielectric constant at selected temperatures. It is apparent from figure 11 that the increase of DC ionic conductivity actually associated with the increase of dielectric constant at different temperatures.



**Figure 9.** Frequency dependence of dielectric constant ( $\epsilon'$ ) for CSC6, at different temperatures.



**Figure 10.** Frequency dependence of bulk dielectric constant ( $\epsilon'$ ) for CSC6 sample, at different temperatures.

It was confirmed that an increase in dielectric constant means an increase in charge carrier concentration [7, 17], and consequently an enhancement in ion transport according to equation (5). The result of this work strongly supports our previous achievements on DC ionic conductivity versus dielectric constant [7, 19, 22], for solid and nanocomposite polymer electrolytes. Thus, similar trends of bulk DC conductivity and bulk dielectric constant (figure 8) with salt concentration and exponential behavior of DC conductivity versus dielectric constants (figure 11) confirmed that the reformulation of Arrhenius equation is required. From the valuable achievements of the current work it is understood that ion transport mechanism is not an easy task and must be considered as a complicated subject in solid polymer electrolytes. The temperature-dependent ionic conductivity for a solid or polymer electrolyte below the glass transition temperature is usually interpreted in terms of Arrhenius equation without any insight into the fundamental mechanisms governing ion transport [7, 27]. In our previous work [7, 22], the dependent of DC ionic conductivity on dielectric constant is confirmed and the reformulated Arrhenius equation [20], is established as follows:

$$\sigma(T, \epsilon') = \sigma_o \exp(-E_a / K_B T \epsilon') \tag{6}$$

From the fundamental point of view, ion transport mechanism in solid polymer electrolytes is complex and depends on factors such as salt concentration and dielectric constant of host polymer [7]. Dielectric constant analysis provides valuable information about the understanding of ion transport in SPEs. The increase of dielectric constant at higher temperatures can be ascribed to the fact that the movement of polymer chain segments and side groups are becomes easier at elevated temperatures and thus the dissociation of ion pairs would increase and resulting in the increase in DC ionic conductivity [7, 19]. The main conclusion in the current work is that the dielectric constant can play a major role in ion transport.

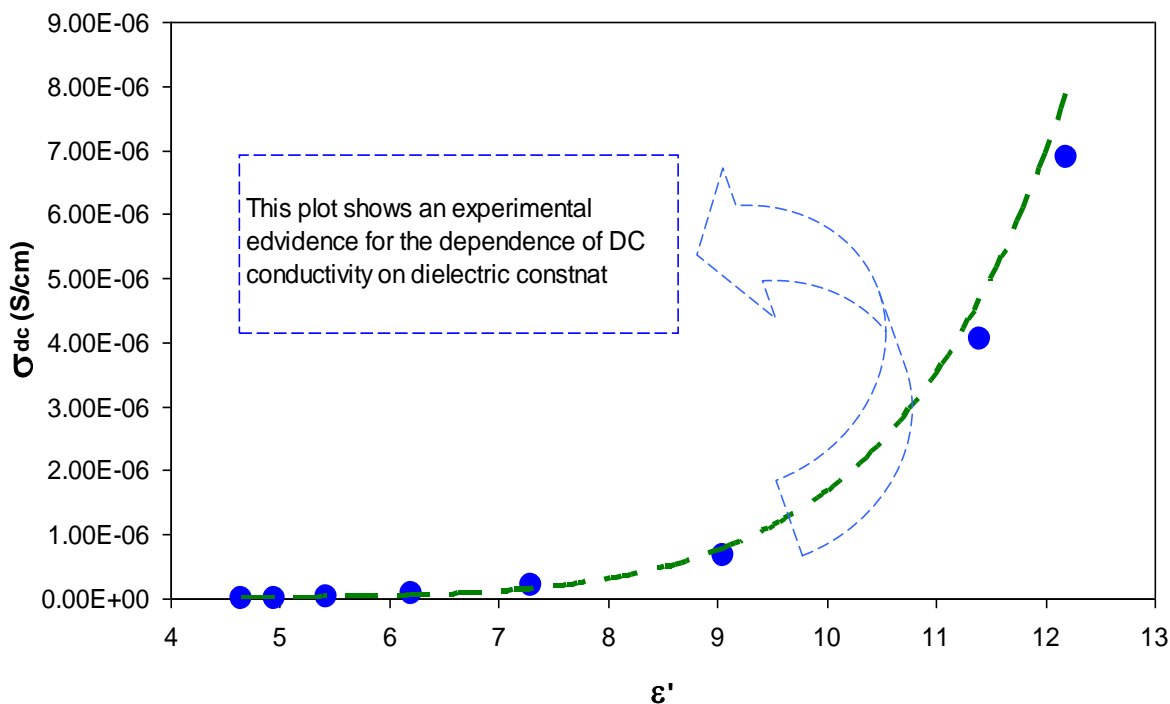


**Figure 11.** DC ionic conductivity versus dielectric constant at temperatures ranges from 303 to 373 K insteps of 10 °C for CSC6 sample.

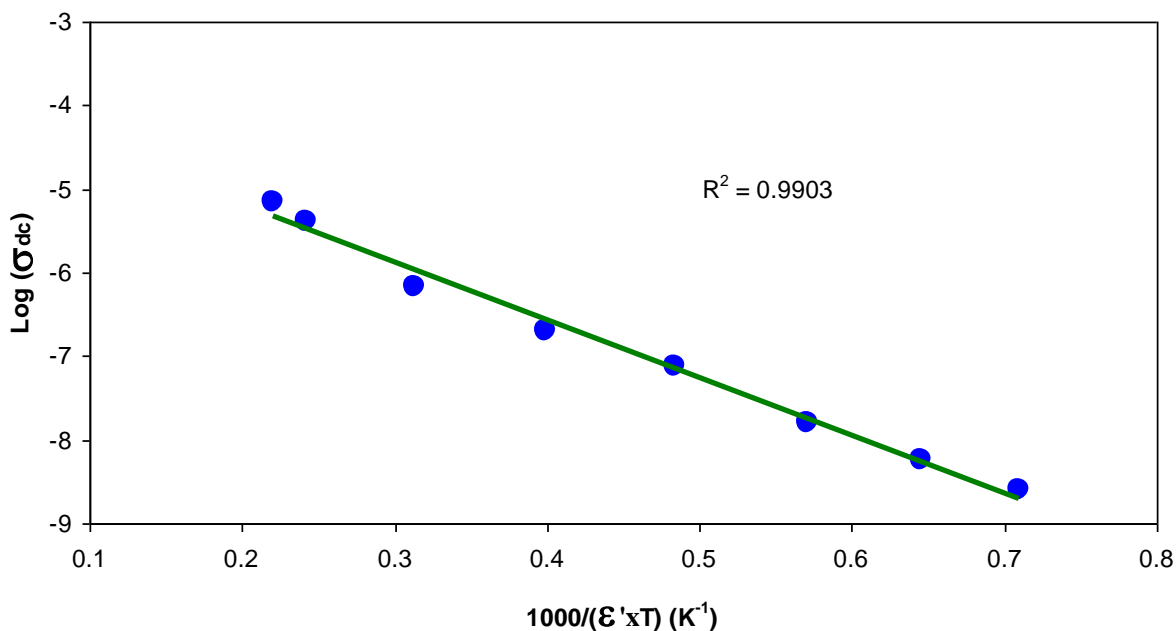


**Figure 12.** DC ionic conductivity versus 1000/(ε'×T) (reformulated Arrhenius equation) for CSC6 sample

For more insights about the reformulated Arrhenius equation the DC conductivity versus 1000/(ε'×T) was plotted for CSC6 sample. The linear behavior of DC conductivity (figure 12) with a  $R^2 = 0.997$  reveals the validity of reformulated Arrhenius equation. The DC conductivity versus

$1000/T$  as exhibited in figure 13, is less linear compared to figure 12 and the regression value is 0.98. Further study and examine more polymer electrolyte systems is needed in this field to support the validity of reformulated Arrhenius equation. The calculated activation energy is 1.36 eV using reformulated Arrhenius equation and is greater than that obtained from Arrhenius equation which is 1.15 eV. Actually polymer electrolytes with lower DC conductivity ( $\approx 10^{-10}$  S/cm) required higher activation energy for ion hopping from one site to another one. Thus the achieved activation energy from reformulated Arrhenius equation is more acceptable.

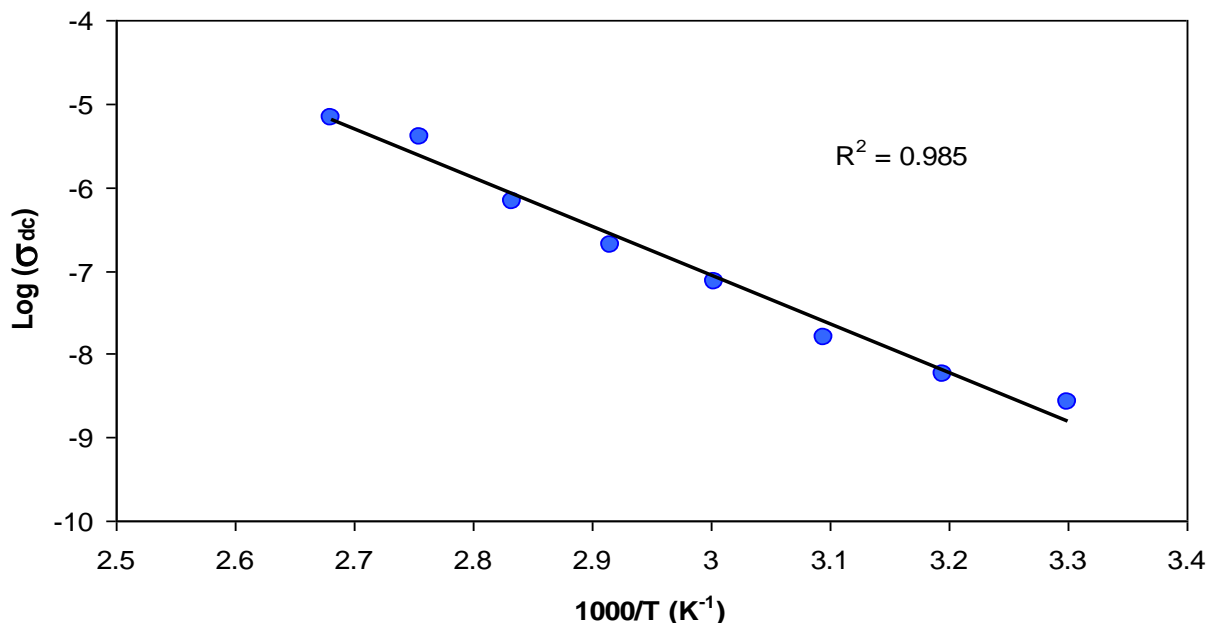


**Figure 13.** DC ionic conductivity versus  $1000/(T)$  (Arrhenius equation)for CSC6 sample

Figure 14 demonstrates the temperature and dielectric constant independent of pre-exponential factor ( $\sigma_0$ ) for CSC6 solid electrolyte sample. Thus the results of CS:LiTf solid electrolyte do not follow the Petrowsky and Frech work [23, 24], which gives a smooth exponential curve between pre-exponential factor and dielectric constant. Consequently, the results of this research work confirm the applicability and satisfactory of reformulated Arrhenius relation [22] in solid polymer electrolytes and reveals the constant behavior of pre-exponential factor. Understanding of fundamental concepts is crucial for the development of Lithium ion batteries (LIBs) as a category of green energy battery which represents the future development direction [5]. Recent studies reveal that Li batteries are most promising energy storage technology for industrialization and it has a wide application in portable electronic devices, electric vehicles, and stationary type distributed power sources [5, 28].

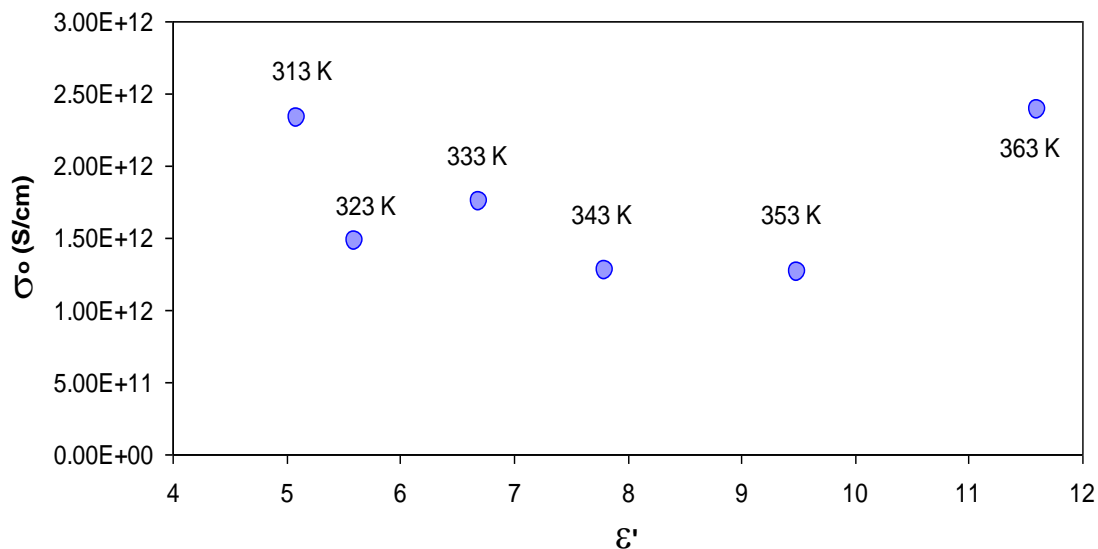


**Figure 14.** Temperature and dielectric constant dependent of pre-exponential factor ( $\sigma_0$ ) at various temperatures for CSC6 system.

#### 4. CONCLUSIONS

In the research work the structural, morphological and ion conduction mechanism in chitosan (CS) based solid polymer electrolyte at low salt concentration was studied. The SEM micrographs of the samples show the smooth surface. The broadening of X-ray peaks of chitosan reveals the reduction of crystalline domain upon LiTf addition and the non existence of any phase separation on the surface (SEM results) of the samples confirms the complexation between chitosan and LiTf salt. The large crystallite size of CSC6 sample reveals the dominance of amorphous portion. In this work the contribution of dielectric constant to Arrhenius equation and its effects on DC conductivity is validated experimentally. The same trend of  $\epsilon'$  and  $\sigma_{dc}$  with salt concentration implies that  $\epsilon'$  study is valuable for predict the conductivity performance of polymer electrolytes. The smooth empirical curve obtained between  $\sigma_{dc}$  and  $\epsilon'$  at different temperature indicates the dependence of DC conductivity on both temperature and dielectric constant,  $\sigma_{DC}(\epsilon', T)$ . The estimated activation energy (1.36 eV) from reformulated Arrhenius equation is higher than one achieved from Arrhenius equation ( $E_a = 1.15$  eV). This informs us that ion hopping in solid polymer electrolytes with lower conductivity requires more energy. The pre-exponential factor is almost constant at different temperature and independent on dielectric constant.

#### ACKNOWLEDGEMENT

The authors gratefully acknowledge the financial support from University of Malaya in the form of grant (grant No. PS214/2009A) for this research project. Shujahadeen Bakr Aziz wishes to thank the Ministry of Higher Education and Scientific Research-Kurdistan Regional Government and University of Human Development for financial supports .

## References

1. N. Boaretto, C. Joost, M. Seyfried, K. Vezzù, V. Di Noto, *J. Power Sources*, 325 (2016) 427-437
2. M. T. Ravanchi, T. Kaghazchi, A. Kargari, *Desalin.*, 235 (2009) 199–244
3. J. S. Kumar, M. J. Reddy, U. V. S. Rao, *J. Mater. Sci.*, 41 (2006) 6171–6173
4. K. Perera, M. A. K. L. Dissanayake, P. W. S. K. Bandaranayake, *Electrochim. Acta*, 45 (2000) 1361–1369
5. J.-Y. Wu, S.-G. Ling, Q. Yang, X.-X. Xu, L.-Q. Chen, *Chin. Phys. B.*, 25 (2016) 078204
6. L. Edman, M. M. Doeff, A. Ferry, J. Kerr, L. C. De Jonghe, *J. Phys. Chem. B.*, 104 (2000) 3476-3480
7. S. B. Aziz, Z. H. Z. Abidin, *J. Appl. Polym. Sci.*, 132 (2015) 41774, DOI: 10.1002/APP.41774
8. M. M. Borgohain, T. Joykumar, S.V. Bhat, *Solid State Ionics*, 181 (2010) 964–970
9. J. Malathi, M. Kumaravadivel, G. M. Brahmanandhan, M. Hema, R. Baskaran, S. Selvasekarapandian, *J. Non-Cryst. Solids*, 356 (2010) 2277–2281
10. G. K. Prajapati, R. Roshan, P. N. Gupta, *J. Phys. Chem. Solids*, 71 (2010) 1717–1723
11. D. K. Pradhan, R. N. P. Choudhary, B. K. Samantaray, *eXPRESS Polym. Lett.*, 2 (2008) 630–638
12. D. K. Pradhan, R. N. P. Choudhary, B. K. Samantaray, *Mater. Chem. Phys.*, 115 (2009) 557–561
13. R. J. Sengwa, S. Choudhary, S. Sankhla, *Compos. Sci. Technol.*, 70 (2010) 1621–1627
14. M. F. Z. Kadir, S. R. Majid, A. K. Arof, *Electrochim. Acta*, 55 (2010) 1475–1482
15. S. B. Aziz, Z. H. Z. Abidin, M. F. Z. Kadir, *Phys. Scr.*, 90 (2015) 035808 (9pp).
16. S. B. Aziz, Z. H. Z. Abidin, *Mater. Chem. Phys.*, 144 (2014) 280-286
17. S. B. Aziz, *Iran. Polym. J.*, 22 (2013) 877–883
18. Z. Osman, Kh. B. M. Isa, A. Ahmad, L. Othman, *Ionics*, 16 (2010) 431–435
19. S. B. Aziz, Z. H. Z. Abidin, *J. Soft Matt.*, Volume 2013, (2013) Article ID 323868, <http://dx.doi.org/10.1155/2013/323868>
20. S. Ramesh, Ch.-W. Liew, K. Ramesh K, *J. Non-Cryst. Solids*, 357 (2011) 2132-2138
21. V. Aravindan, C. Lakshmi, P. Vickraman, *Curr. Appl Phys.*, 9 (2009) 1106–1111
22. S. B. Aziz, *Adv. Mater. Sci. Eng.*, Volume 2016 (2016), Article ID 2527013, <http://dx.doi.org/10.1155/2016/2527013>
23. M. Petrowsky, R. Frech, *J. Phys. Chem. B.*, 113 (2009) 5996-6000
24. M. Petrowsky, R. Frech, *Electrochim. Acta*, 55 (2010) 1285-1288
25. S. Bureekaew, S. Horike, M. Higuchi, M. Mizuno, T. Kawamura, D. Tanaka, N. Yanai, S. Kitagawa, *Nat. Mater.*, 6 (2009) 831-836
26. P. B. Bhargav, V. M. Mohan, A. K. Sharma, V. V. R. N. Rao, *Curr. Appl Phys.*, 9 (2009) 165–171
27. M. Petrowsky, R. Frech, *J. Phys. Chem. B.*, 114 (2010) 8600–8605
28. X. Yao, B. Huang, J. Yin, G. Peng, Z. Huang, C. Gao, D. Liu, X. Xu, *Chin. Phys. B*, 25 (2016) 018802